



ELSEVIER

Available online at [www.sciencedirect.com](http://www.sciencedirect.com)

SCIENCE @ DIRECT®

Nuclear Instruments and Methods in Physics Research A 545 (2005) 252–260

NUCLEAR  
INSTRUMENTS  
& METHODS  
IN PHYSICS  
RESEARCH  
Section A

[www.elsevier.com/locate/nima](http://www.elsevier.com/locate/nima)

# Radiation monitoring in Mrad range using radiation-sensing field-effect transistors

S. Stanič<sup>a,\*</sup>, Y. Asano<sup>a</sup>, H. Ishino<sup>b</sup>, A. Igarashi<sup>a</sup>, S. Iwaida<sup>a</sup>, Y. Nakano<sup>a</sup>,  
H. Terazaki<sup>a</sup>, T. Tsuboyama<sup>c</sup>, I. Yoda<sup>b</sup>, D. Žontar<sup>d</sup>

<sup>a</sup>University of Tsukuba, Tennodai 1-1-1, Tsukuba 305-8573, Japan

<sup>b</sup>Tokyo Institute of Technology, Oh-Okayama, Tokyo 152-8551, Japan

<sup>c</sup>KEK, High Energy Accelerator Research Organization, Oho 1-1, Tsukuba 305-0801, Japan

<sup>d</sup>Jozef Stefan Institute, Jamova 39, Ljubljana, Slovenia

Received 13 September 2004; received in revised form 17 January 2005; accepted 19 January 2005

Available online 19 April 2005

## Abstract

In many of the recent  $e^+e^-$  particle physics experiments, monitoring of the accumulated dose in silicon is essential to maximize the lifetime of silicon vertex detectors operating in severe radiation environments. Using radiation-sensing field-effect transistors (RadFET) as radiation monitoring devices, we studied their responses during irradiation and during subsequent annealing. The relation between the RadFET response and the dose was determined by irradiations with a  $^{60}\text{Co}$  source with known activity. The study of annealing at three different temperatures showed that RadFETs gradually anneal for up to 40%. Annealing can be fitted by a sum of two exponential functions with time constants of 3 and 85 days.

© 2005 Elsevier B.V. All rights reserved.

PACS: 07.85.Qe; 85.30.Tv

Keywords: B factory; Radiation monitoring; Silicon detectors; Annealing

## 1. Introduction

Radiation from beam induced backgrounds that strikes silicon tracking and vertexing detectors

(SVD) close to the interaction region was found to be a serious problem in certain high luminosity  $e^+e^-$  particle physics experiments [1,2]. Since the performance of those detectors decreases with accumulated dose, mainly due to gain drop of the read-out electronics, feedback to accelerator operation is necessary to increase the SVD lifetime. As a candidate for on-line radiation

\*Corresponding author. Tel./fax: +81 29 853 6787.

E-mail address: [stanic@beauty.bk.tsukuba.ac.jp](mailto:stanic@beauty.bk.tsukuba.ac.jp) (S. Stanič).

<sup>1</sup>On leave from Nova Gorica Polytechnic, Slovenia.

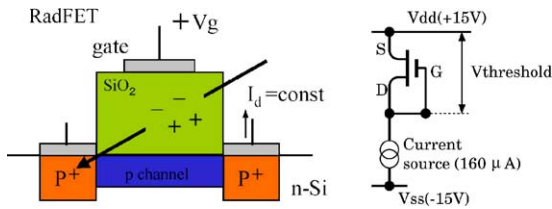


Fig. 1. Schematic view of a p-type RadFET (left) and its read-out (right).

monitors up to several Mrad of accumulated dose in silicon, we investigated the electrical properties of radiation sensing p-channel metal-oxide-semiconductor field-effect transistors [3,4], referred to in the further text as RadFET. When ionizing radiation passes through the metal-oxide structure (Fig. 1, left), the deposited energy creates electron–hole pairs. After some initial recombination, the electrons are quickly swept out of the oxide. A fraction of holes is during their relatively slow transport through the oxide trapped in the oxide defects, which can retain them for long periods of time at room temperature [5]. This trapped charge shifts the value of the gate threshold voltage, required to maintain a given constant drain current through the transistor. Connecting the gate of each transistor to its drain (Fig. 1 right) ensured the p-MOSFET operation in saturation mode, where the relation between the square root of the drain current and gate voltage is linear and unaffected by the gate-drain bias voltage [6]. The relation between the gate voltage shift and the dose heavily depends on the production process parameters, especially on the thickness of the gate oxide, and has to be determined experimentally, using a calibrated radiation source. Since there is very limited space in the Belle detector,  $1 \times 1 \times 1 \text{ mm}^3$  bare RadFET chips<sup>2</sup> were used. Each chip contains four transistors, two with sensitivity in rad range (R) and two with sensitivity in krad (K) range. Physical difference between R and K transistors is in the thickness of the oxide layer, which is 0.95 and 0.13 μm, respectively [7]. The accumulated doses of interest for our purposes were on the level of several Mrad, so only K transistors in each chip were used.

<sup>2</sup>Product of REM Oxford Ltd., Oxford, UK.

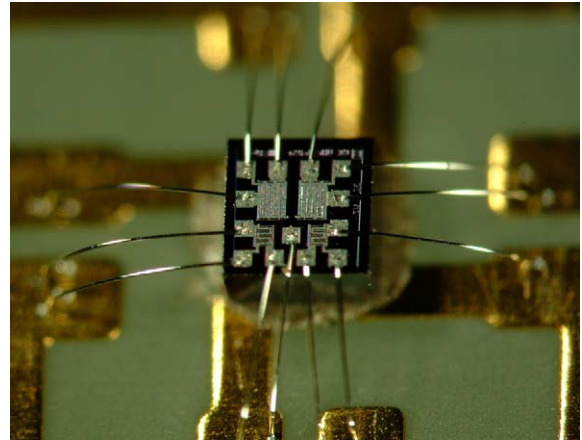


Fig. 2. A mounted RadFET chip. The two K range transistors it contains are electrically connected to the readout circuit by wire bonds. The chip's dimensions are  $1 \times 1 \times 1 \text{ mm}^3$ .

## 2. Irradiation

Bare RadFET chips were glued to a printed circuit support board and electrically connected by bonding wires (Fig. 2). The operating drain current of the transistors was set to 160 μA based on previous measurements [7,8] and was maintained by a constant current source with stability of less than  $10^{-3}$ . We confirmed that the temperature dependence of the gate voltage at 160 μA (Fig. 7) is small enough for our application both for non-irradiated transistors ( $\sim 0.5 \text{ mV/K}$ ) and for those irradiated to 1.85 Mrad ( $\sim 2.5 \text{ mV/K}$ ). The applicable gate threshold voltage range in our setup was from +12.5 to  $-8 \text{ V}$ . Gate voltages were read out during a 2 ms long pulse, which was periodically sent once every 1 or 2 min. For the remaining time, the source and drain of the transistors were electrically shorted. To monitor the temperature, a PT100 temperature sensor was also included in the setup. Gate voltages and temperatures were logged by a data logger<sup>3</sup> and stored in a PC computer. The support containing the RadFETs was glued to a 3 cm thick lead block, with the chips facing the source and no other material between the chips and the source (Fig. 3). In denser materials photons develop Compton-

<sup>3</sup>DA-100, Yokogawa Electric Corporation, Japan.

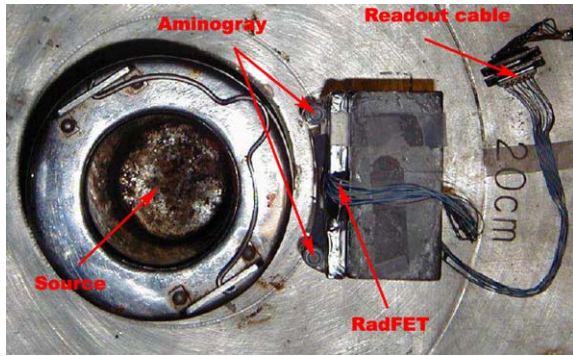


Fig. 3. Positioning of RadFET samples and Aminogray dosimeters at  $^{60}\text{Co}$  source. “20 cm” line in the figure denotes 20 cm distance from the center of the source. The cable connected to the sensors goes through the wall of irradiation chamber to the readout.

scattered electrons, which could affect the dose in silicon oxide. To check if Compton-scattered electrons affect the RadFET response, half of the RadFET in one of the irradiations were shielded by a 2 mm thick Al plate (Fig. 4). RadFET chips were irradiated by a calibrated  $^{60}\text{Co}$   $\gamma$ -ray source.<sup>4</sup>  $^{60}\text{Co}$  emits  $\gamma$ -rays with  $E = 1.17\text{ MeV}$  (50%) and  $1.33\text{ MeV}$  (50%), and has a half life time of 5.27 years. Since the irradiations took at most a few days, we assumed the source activity to be constant during each irradiation. Based on the source activity, the absorbed dose in silicon was calculated as a function of the distance from the source. Two types of irradiation were performed, “fast” irradiation experiments with dose rates about 80 krad/h, where the distance from the source was 10 cm, and a “slow” experiment with the rate about 1.6 krad/h 70 cm away from the source. In the fast dose rate case, the main uncertainty in the calculated dose stemmed from the positioning precision of the samples (Fig. 3). A 5 mm positioning error, which was our precision, yielded a 10% error in the dose. In the case of a slow dose rate the 5 mm positioning error yielded only a 1.5% error in the dose. The calculated dose was verified by commercial aniline-based (Aminogray) dosimeters,<sup>5</sup> placed as close to the RadFET

chips as possible (Fig. 3). The precision of Aminogray dose measurement is 1% [10,11], however, there is an additional 10% error due to the relative positioning of the Aminogray with respect to the RadFET sensors. In all irradiations the doses measured by Aminogray agree with the calculated ones within the estimated errors. For the final doses, a 10% error was assumed. Dosimetry details are summarized in Tables 1 and 2.

### 3. Results

The primary goal of the study was to establish whether the K range RadFET can be used for radiation monitoring up to several Mrad, and to experimentally determine the relation between dose and transistor gate voltage. The relevant quantity is not the absolute gate threshold voltage itself but the shift of the gate threshold voltage from its original, non-irradiated value (threshold shift). For the sake of convenience we defined it as a positive quantity

$$V_{\text{shift}}(t) = -(V_{\text{threshold}}(t) - V_{\text{threshold}}(t = 0)).$$

$V_{\text{shift}}$  is independent of the details of the readout system, as long as the current through FET is kept constant. In the subsequent text and figures the threshold shift will be used instead of the absolute FET gate voltage. Since the charge trapping processes in silicon oxide may depend on the applied dose rate [4], we performed both “fast” irradiations at high dose rates and a “slow” irradiation at a low dose rate. Fast and slow irradiations required two conceptually very different approaches. In the fast case, we wanted the dose rate to be as high as possible. It was limited at around 80 krad/h by the source configuration and activity (Fig. 3). Each fast irradiation was completed in a single step with continuous read-out and logging of the RadFET response. In order to understand the annealing effects, the measurements continued after the irradiation. In the slow case, we wanted to study RadFET behavior up to the same dose as in the fast one, but at a dose rate 50 times lower. The longer irradiation had to be performed in 7 steps, each requiring about 5 full

<sup>4</sup>Located at Tokyo Institute of Technology, Tokyo, Japan.

<sup>5</sup>Product of HITACHI Cable Co., Japan.

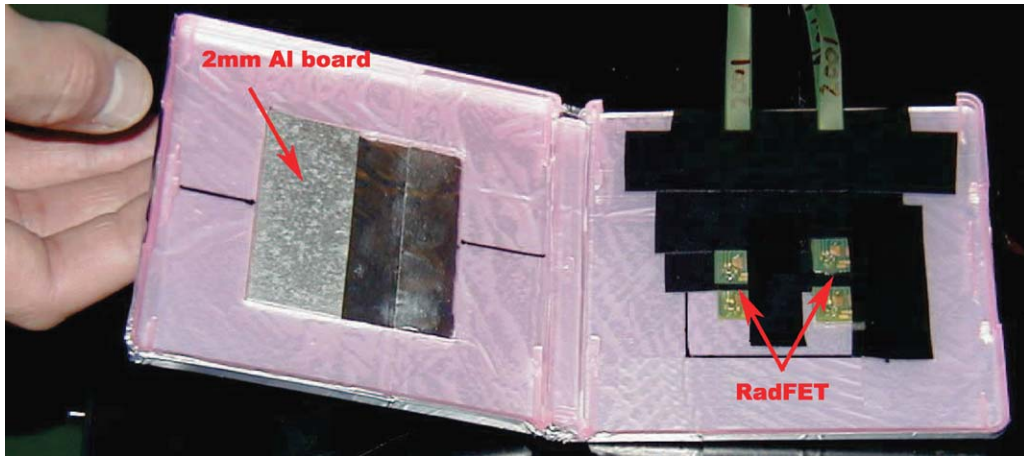


Fig. 4. RadFETs for irradiation. Half of the chips were shielded by a 2 mm thick Al plate, which served as a Compton scatterer.

Table 1

Summary of irradiations at high dose rates with corresponding  $^{60}\text{Co}$  source activities, irradiation times, doses taken by the RadFET and dose rates

Irrad. No.	Activity (TBq)	Irrad. time (h)	Calc. dose (krad)	Meas. dose (krad)	Calc. rate (krad/h)	Meas. rate (krad/h)
Fast 1	25.3	5.20	448	478	86.1	92.0
Fast 2	23.7	5.58	450	481	80.6	86.2
Fast 3	22.2	25.63	1935	2117	75.5	82.6
Fast 4	20.2	29.47	1856	1621	63.0	55.0

Calculated values are based on the source activity and distance. The measured values are based on Aminogray dosimetry. For all doses a 10% error is implied.

Table 2

Summary of the low dose rate ( $\sim 1.6$  krad/h) irradiation, performed in 7 steps

Irrad. step	1	2	3	4	5	6	7
Calc. dose (krad)	100	500	700	900	1100	1300	1500
Meas. dose (krad)	98	551	813	1057	1324	1379	1466

Calculated values are based on the source activity. The measured values are based on Aminogray dosimetry. For all doses a 10% error is implied.

days of exposure. The RadFETs were irradiated without on-line readout, with source, gate and drain of the transistors electrically shorted, and after each step were left to anneal for 10 days at

room temperature before the gate threshold shift was measured.

Results of the above experiments are as follows. We confirmed that K range RadFET sensors can survive doses up to 2 Mrad, where the threshold shift increased to about 11 V. The threshold shift as a function of dose agreed within estimated errors for all fast irradiations performed (Fig. 5, left), as well as for the slow irradiation (Fig. 6). Its inverse, dose as a function of the threshold shift, can be in the range from 0 to 2 Mrad parameterized by a second-order polynomial as

$$\text{Dose} = 32V_{\text{shift}} + 12V_{\text{shift}}^2.$$

In the above relation, the dose is measured in krad and the threshold shift in volts. In each fast

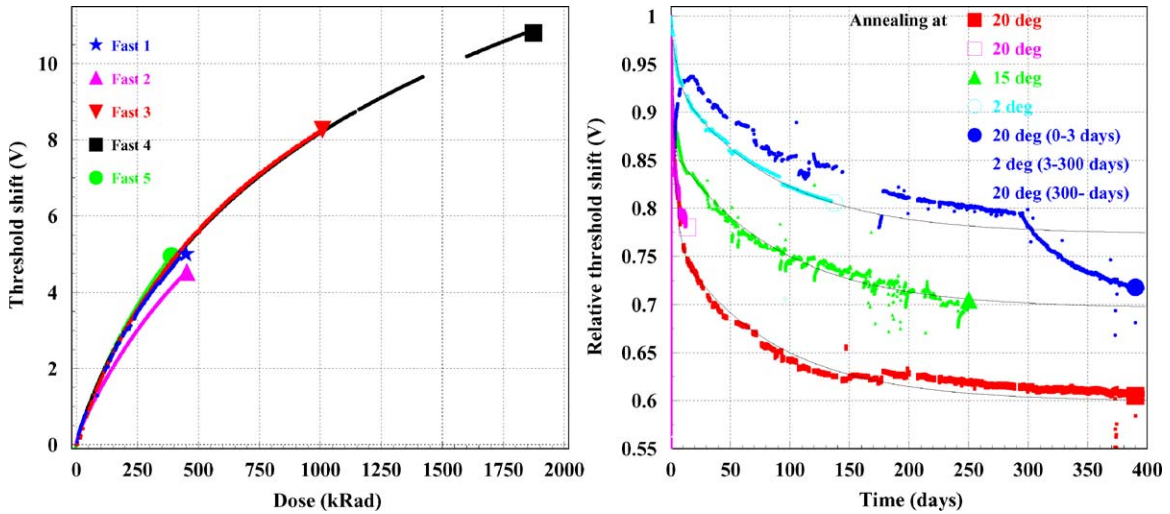


Fig. 5. Left: threshold shift as a function of dose during irradiations at high dose rate. Right: threshold shift as a function of annealing time, fitted by a sum of two exponential functions. Parameters of the fit are given in Table 3. Annealing at 20–30 °C is denoted by red squares, at 15 °C by green triangles and at 2 °C by blue circles. Total annealing and annealing speed decrease with temperature. Behavior of the topmost curve is due to two temperature changes at 3 and 300 days after irradiation. Resulting reverse annealing and increase of the annealing can be seen.

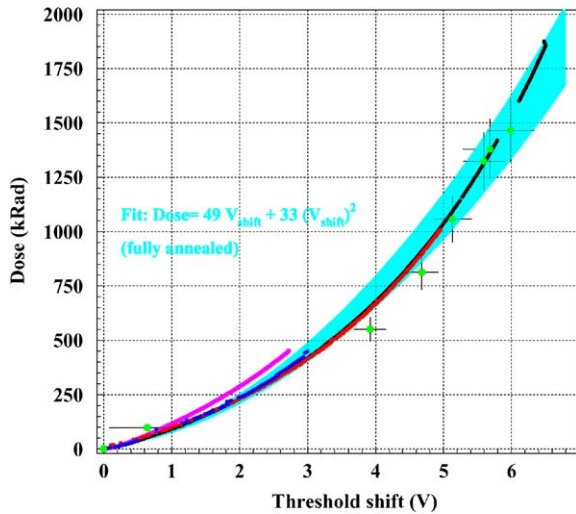


Fig. 6. Accumulated dose in RadFET as a function of the threshold shift. The curves with many data points represent high dose rate data, and the single points with large error bars low dose rate data. The shaded area is a fit with an assumed 10% error in dose.

irradiation 4–8 K range RadFET sensors were exposed. The responses of individual sensors slightly differ from chip to chip, whereas the

responses of the two FET on the same chip are practically identical. We attribute this to the slightly different accumulated doses due to the positioning error (Fig. 3) and to the variation of oxide layer thickness between chips. The threshold shift spread between the sensors is treated as a systematic error for each measurement. In the irradiation where half of the chips were shielded by the Al plate that induced Compton scattering, we observed no difference in the voltage dependence between the shielded and the non-shielded chips.

### 3.1. Annealing

A fraction of holes, created in the RadFET oxide layer by the incident ionizing radiation, remain at room temperatures permanently trapped within the oxide. Holes captured within 2–5 nm distance from the silicon represent the majority of the trapped charge. The detrapping of these shallow oxide states, mostly via Fowler–Nordheim tunneling of electrons from Si, was found to be primarily responsible for the long-term annealing. Another annealing component originates from the detrapping of the deeper oxide states via stochastic

hopping mechanisms. Both types of processes are expected to show exponential time dependence of the annealing [5]. In the scope of the presented experiment we tried to determine the magnitude and time constants of the threshold shift recovery and to gather information about their dependence on the storage temperature. Our measurements provide some information about the annealing processes on a time scale of up to two years and for temperature range between 2 and 25 °C.

The observed fast recovery immediately after the irradiation and slow recovery continuing for more than a year (Fig. 5, right) suggested at least two underlying annealing processes, so the data was fitted by a sum of two exponential functions with different time constants:

$$V(t) = V_{\max} + V_{\text{fast}}e^{-t/\tau_{\text{fast}}} + V_{\text{slow}}e^{-t/\tau_{\text{slow}}}$$

where  $V_{\max}$  is the threshold shift of a fully annealed transistor and  $V(0)$  is the maximal threshold shift immediately after irradiation.  $V_{\max}$  accounts for the fact that the RadFETs did not anneal to their pre-irradiation values and some gate voltage shift remained permanently. To be able to compare the data from different experiments,  $V(0)$  was in each one of them normalized to 1. The fitting itself was performed by the MINUIT package [9] using the least  $\chi^2$  method. Amplitudes and time constants of the exponential decays were kept as free parameters of the fit, and the constant term  $V_{\max}$  was constrained to  $V_{\max} = V(0) - V_{\text{fast}} - V_{\text{slow}}$ . Results of the fit to the threshold voltage shift data from RadFETs stored constantly at 3 different temperatures: 2, 15 and 20 °C are summarized in Table 3.

The annealing speed and the total amount of annealing were found to decrease with storage temperature after irradiation. Assuming that two annealing processes govern the recovery of the threshold voltage shift in the investigated time interval and temperature range, the corresponding decay time constants have been found to be

$$\tau_{\text{fast}} = 3(1 \pm 0.5) \text{ days and } \tau_{\text{slow}} = 85(1 \pm 0.1) \text{ days.}$$

In one of the experiments, annealing at different temperatures was studied using RadFETs exposed to the same dose in the same irradiation (Table 1, Fast 4). They were divided into 2 groups after annealing together for 3 days at room temperature, one of them remaining at 20 °C and the other kept constantly below 2 °C. As a result, the annealing rate of the RadFETs kept at 2 °C significantly decreased, and for about 2 weeks after the temperature change reverse annealing could be seen. The threshold gate voltage shift of these RadFETs recovered for about 20% less than in the case of annealing at 20 °C. After about 300 days of annealing, when the short component seemed to disappear completely, the temperature was increased from 2 to 15 °C. The annealing speed and magnitude increased as well, but the data did not correspond to annealing with  $\tau_{\text{fast}} = 3$  days. It could be described almost entirely by a single exponential with  $\tau' = 43$  days, which suggested fitting the threshold voltage shift with 3 instead of 2 exponential functions. The same fitting procedure as before was applied, yielding  $\tau_{\text{fast}} \approx 4$  days,  $\tau_{\text{med}} \approx 40$  days and  $\tau_{\text{slow}} \approx 400$  days for the 20 °C data. Nice agreement of  $\tau_{\text{med}}$  and  $\tau'$  suggests that some annealing process with this

Table 3  
Results of the fit

Temp. (°C)	$V_{\max}/V(0)$	$V_{\text{fast}}/V(0)$	$\tau_{\text{fast}}$ (days)	$V_{\text{slow}}/V(0)$	$\tau_{\text{slow}}$ (days)
2	0.77	0.07	4.8	0.16	84.9
15	0.69	0.14	1.3	0.17	87.8
20	0.60	0.23	3.4	0.17	83.9

The total threshold voltage shift decrease at after annealing (column 2) increases with temperature. Weights of the exponential components of the fit are given in columns 3 and 5. The decay times are given in columns 2 and 6. For all parameters a 5% error is implied.  $\chi^2/\text{ndf}$  of the fit is in all cases less than 1.

time constant is present at all temperatures, but for a reliable description longer measurements of annealing at low temperatures are needed, as well as systematic studies of the temperature change effects.

Behavior of the threshold shift at various annealing temperatures suggests that below a certain temperature the fast annealing processes become partially or fully suspended, while the slow processes keep on going. When the temperature increases, the fast annealing processes seem to resume as well. Furthermore, soon after irradiation, threshold shift changes were observed during short time temperature cycles as small as 1 °C around the 2 °C storage temperature, which also suggested that the threshold temperature for suspension of the fast annealing process might be close to 2 °C.

Another important issue is the comparison of high and low dose rate results. To correctly compare the threshold shifts, RadFETs must in both cases be at the same stage of annealing. However, the threshold shift data from fast irradiations is without any annealing, and the voltage drops measured after each step of the slow irradiation includes some annealing at room temperature. The most reasonable choice is to compare the threshold shift versus dose curves after sensors were fully annealed, as this is the only stable state where threshold shifts no longer change. The problem with this choice is that RadFET need about a year to fully anneal, which cannot be done at each step of the slow irradiation if the measurement is to be carried out in reasonable time. We therefore decided to let the RadFETs from the slow irradiation anneal for only about 10 days at room temperature, during which the fast annealing almost completely died out, measure their threshold shifts and then irradiate them again. According to the measured annealing curve (Fig. 5, right), they should have annealed to about a half of the final value. To reach complete annealing for all data points, we multiplied the fast irradiation threshold shift data (Fig. 5, left) by 0.6 and the slow irradiation data by 0.77, as shown in Fig. 6. No significant difference between the high and the low dose rate data was observed. A fit of a second-order polynomial to

the average of fully annealed data from all experiments yields

$$\text{Dose} = 49V_{\text{shift}} + 33V_{\text{shift}}^2$$

where the dose is measured in krad and the threshold shift in volts.

We also investigated how the gate voltage of a RadFET responds to a slow ( $\sim 1$  °C/h) temperature change in the 5–25 °C range. We found that the RadFET response follows 3 basic patterns. In a non-irradiated RadFET, there is practically no voltage variation. For a fully annealed transistor this variation is small, but the increase of the gate voltage with temperature can nevertheless be clearly seen even for a RadFET after 2 years of annealing at room temperature. For a RadFET in an early stage of annealing the gate voltage strongly varies with the temperature. In all the measurements within the first 2 months of annealing a clear peak in the sensor response can be seen at around 11–18 °C (Fig. 7). Since each RadFET has a slightly different absolute gate voltage, the voltage difference

$$\Delta V = V_{\text{gate}}(T) - V_{\text{gate}}(T_{\text{min}})$$

is plotted for easier comparison. With time, the peak gradually decreases and shifts to higher temperatures and finally disappears. The measured temperature variation effect shows a strong correlation with the fast component of the annealing, but more systematic studies are needed to draw definite conclusions.

#### 4. Conclusion

To summarize, K range RadFETs were found to be suitable for dosimetry purposes up to at least 2 Mrad. In this dose range, the relation between dose and gate threshold shift during irradiation can be parameterized as

$$\text{Dose} = 32V_{\text{shift}} + 12V_{\text{shift}}^2$$

where the dose is measured in krad and the threshold shift in volts. During irradiation with  $^{60}\text{Co}$ , we observed no change in RadFET response

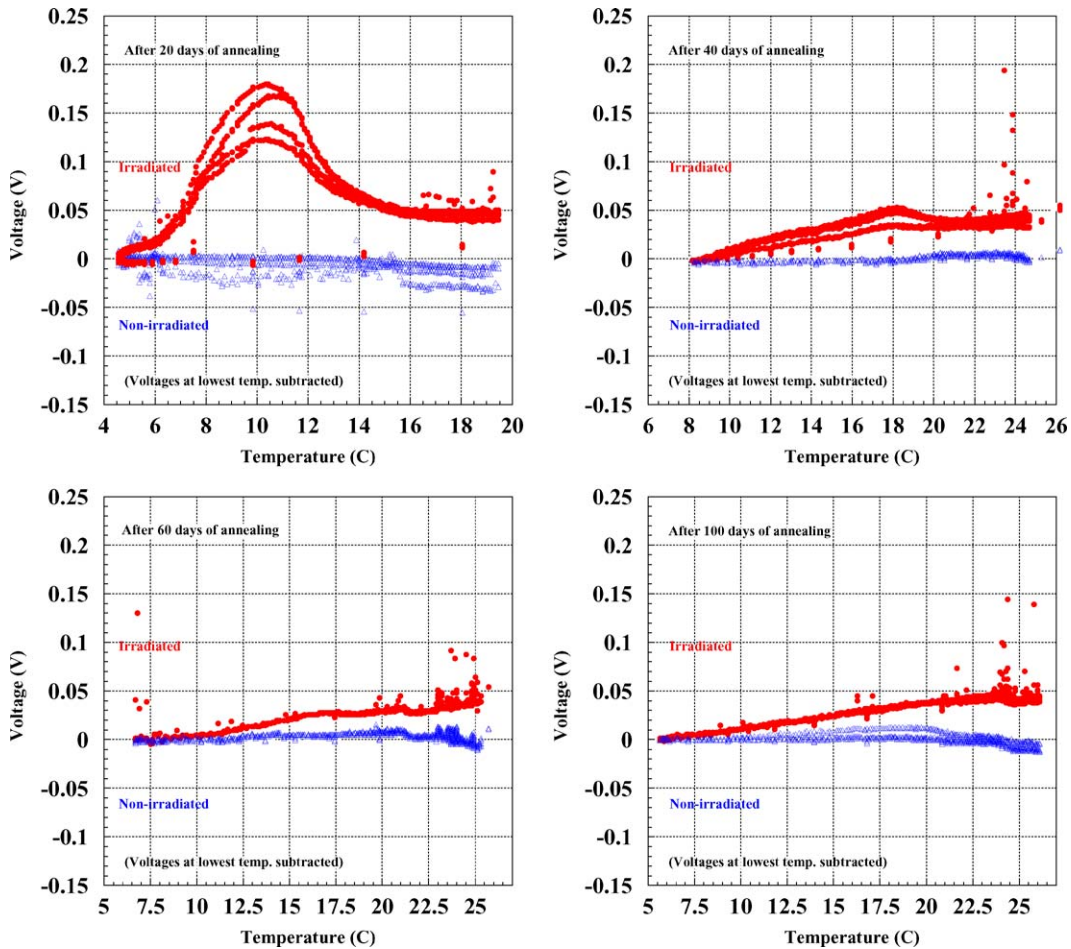


Fig. 7. Temperature dependence of the gate voltage at constant current for irradiated (full circles) and non-irradiated (open triangles) RadFETs after 20, 40, 60 and 100 days of annealing. Irradiated RadFETs were exposed to 1.85 Mrad. For easier comparison of various sensors, the gate voltage difference from the lowest temperature point is plotted.

with or without a 2 mm thick Al Compton scatterer between the sensors and the source. After irradiation, the threshold shifts at room temperature gradually annealed for about 40%. The annealing can be fitted by a sum of two exponential functions with decay times of 3 and 85 days. The fast component strongly depends on the temperature and is in the early stage strongly suppressed below 2°C. The relation between the RadFET gate voltage and the chip temperature differs for a non-irradiated RadFET, for a fully annealed irradiated one and for a recently irradiated one. Its behavior suggests

strong correlation with the fast component of the annealing.

### Acknowledgements

For the help with the production and selection of RadFET chips we wish to thank A. Holmes-Siedle of REM Oxford Ltd., Oxford, United Kingdom. For initial designs of a RadFET reader and a working device, with which we did most measurements we are indebted to A.B. Rosenfeld of Wollongong University, Australia.

**References**

- [1] A. Abashian, et al., Nucl. Instr. and Meth. A 479 (2002) 117.
- [2] B. Camanzi, et al., IEEE Trans. Nucl. Sci. NS-49 (2002) 1275.
- [3] A. Holmes-Siedle, Nucl. Instr. and Meth. 121 (1974) 169.
- [4] A. Holmes-Siedle, A Handbook of Radiation Effects, Oxford UP 134, 2001.
- [5] T.P. Ma, P.V. Dressendorfer, Ionizing Radiation Effects in MOS Devices and Circuits, Wiley, New York, 1989.
- [6] M.G. Buehler, B.R. Blaes, G.A. Soli, G.R. Tardio, On-chip P-MOSFET Dosimetry, IEEE Trans. Nucl. Sci. NS-40 (1993) 6.
- [7] A. Holmes-Siedle, REM's Integrating Dosimeter System Based on the RadFET, REM-TR 98-3, REM Oxford Ltd., 1999.
- [8] A.B. Rosenfeld, A system for radiation damage monitoring, IEEE Trans. Nucl. Sci. NS-46 (1999) 6.
- [9] F. James, MINUIT—function minimization and error analysis, CERN Program Library D506, 1988.
- [10] Aminogray specification sheet, Hitachi Cable Co.
- [11] T. Kojima, et al., Alanine Dosimeter Molded with Polystyrene, JAERI-M 86-137, 1986.